



Heat Treatment of Mg-Containing Aluminum Alloys 5182 and 6016 in an Oxidizing Atmosphere with 4% CO₂

Cathrine Kyung Won Solem, Per Erik Vullum, Gabriella Tranell, and Ragnhild E. Aune

Abstract

Oxidation of liquid aluminum (Al) during processing is a widely known problem, and magnesium (Mg), as a common alloying element, increases the oxidation rate of the alloy. It has been established that small additions of CO₂ ($\geq 4\%$) in an oxidizing atmosphere have a significant inhibiting effect on the rate of oxidation of Al alloys 5182 (AlMg4.5Mn0.4) and 6016 (AlSi1.2Mg0.4) discs based on oxide layer thickness and mass gain when heat-treated at 750 °C for 7 h. The phases present in the oxide layers for each alloy have now been identified and compared with discs heated in synthetic air and argon (Ar) under the same experimental conditions. The XRD analyses revealed the presence of MgO for all Al alloy 5182 discs, in addition to MgAl₂O₄ and Al₂O₃ when heated in synthetic air, and Mg₂C₃ when heated in the mixed cover gas containing 4% CO₂. The low Mg-containing Al alloy 6016 revealed the presence of MgAl₂O₄ for all discs, in addition to MgO when heat-treated in the mixed cover gas containing 4% CO₂, as well as Al₂O₃ when heated in Ar. For both alloys, Transmission Electron Microscopy (TEM) combined with Energy Dispersive X-ray Spectroscopy and Electron Energy Loss Spectroscopy (EDS-EELS) analyses revealed that the mixed cover gas also resulted in a nanometer-thin amorphous C layer, never previously detected, on top of the thin nanocrystalline MgO layer, retarding the evaporation of Mg and inhibiting the oxidation rate for both alloys.

C. K. W. Solem (✉) · G. Tranell · R. E. Aune
Department of Materials Science and Engineering, Norwegian University of Science and Technology (NTNU), Trondheim, Norway
e-mail: cathrine.k.w.solem@ntnu.no

P. E. Vullum
Department of Physics, Norwegian University of Science and Technology (NTNU), Trondheim, Norway

P. E. Vullum
SINTEF Industry, Trondheim, Norway

Keywords

Aluminum • Oxidation • MgO • CO₂

Introduction

Aluminum (Al) and its alloys are a necessity in modern society and as today's second most important metal, Al is on its road to becoming an even more sustainable and renewable material [1]. Challenges related to production and processing of Al, i.e. oxidation and metal loss, have been a topic of interest for over a century [2] and several studies have been carried out trying to understand the overall mechanisms of oxidation of Al and typical alloying elements like Mg [2–4]. Even the behavior and onset of breakaway oxidation leading to the formation of less protective phases such as spinel (MgAl₂O₄) in the case of Mg-containing Al alloys have been studied in detail [2–4].

Inhibition of Oxidation by CO₂

The literature contains several studies in regard to inhibition of the oxidation of Al, as well as how the rate of oxidation may be delayed and hindered [5–7]. Based on these studies, it has been established that the chemical composition and the oxidizing atmosphere are parameters influencing the system. An example is the case of Al–Mg alloys, where it has been established that the Mg content influences the rate and extent of oxidation, which may be inhibited if the oxidation step forming MgO is retarded [8–10].

It is a well-known fact that as the Gibbs energy of formation for MgO is lower than for Al₂O₃, the oxygen present in the atmosphere generates MgO as the stable phase. It was, however, demonstrated by Smith et al. in 2019 that small additions of CO₂ in the oxidizing atmosphere of Al–Mg systems had a significant influence in regards to the rate of

oxidation [10]. It was observed in their study that the CO_2 in the cover gas was adsorbed on top of the MgO layer formed on the surface of the Al–Mg alloy, preventing further diffusion of Mg through the MgO layer, hence, inhibiting the rate of oxidation [10]. Similarly, CO_2 has been studied and found to have an important role in aqueous solutions, preventing oxidation and corrosion of Mg alloys due to the formation of insoluble products acting as a protecting film on the surface [11].

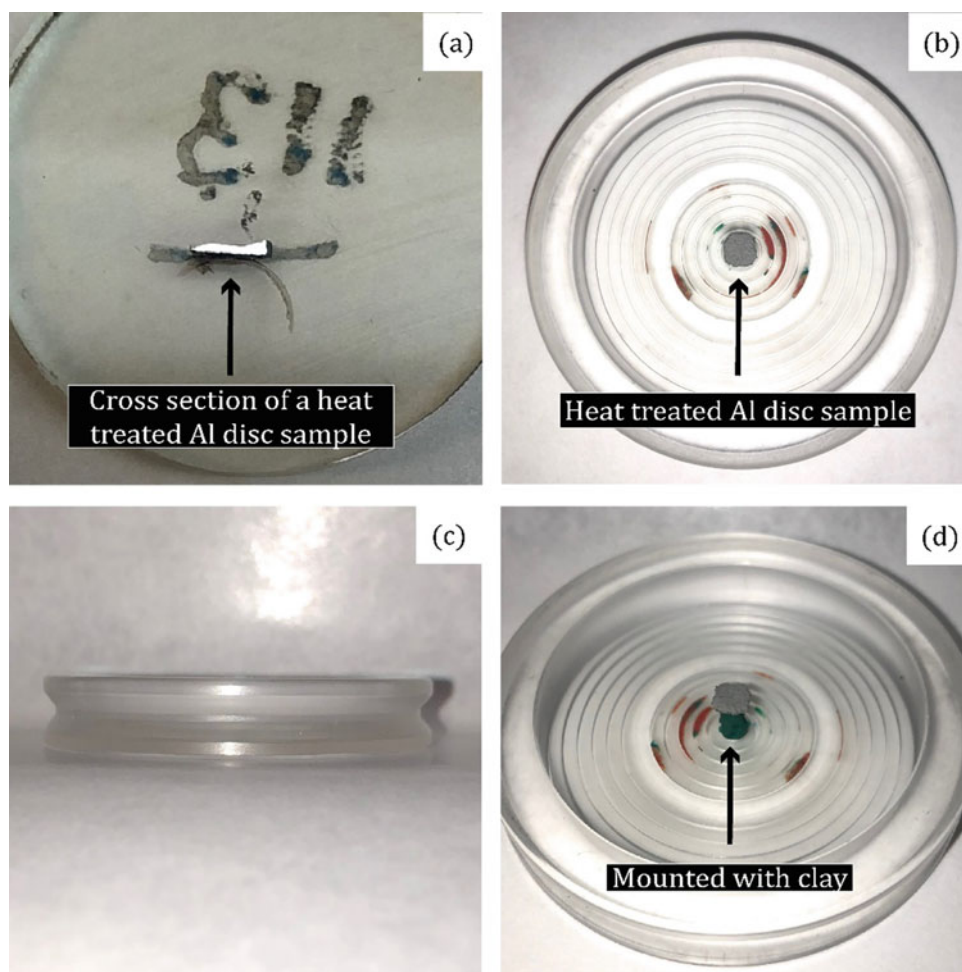
Several mechanisms on how the CO_2 and MgO surfaces interact have been proposed, and the behavior of CO_2 when physisorbed, e.g. adsorbed to the surface by van der Waals forces at an already existing MgO surface, has also been investigated by Tosoni et al. [12]. Based on their findings, they suggest that a carboxylate complex or a carbonate, i.e. CO_2^- or CO_3^{2-} , may be the compounds present on the MgO surface. Alkali earth metal oxides in general, e.g. MgO and CaO , have been reported to be suitable recipients to CO_2 [13], however, only for specific crystal orientations, e.g. orientation (100) in the case of MgO .

The present authors have previously studied the oxidation steps experienced by Al–Mg alloys in the casthouse during

Al production, by exposing high and low Mg-containing alloys to different cover gases in controlled laboratory environments [9]. In this study, Al discs of the alloys 5182 (AlMg4.5Mn0.4) and 6016 (AlSi1.2Mg0.4) were heat-treated at 750 °C for 7 h in three different cover gases: (i) 80% synthetic air and 20% Ar, (ii) 99.999% Ar, and (iii) 4% CO_2 , 76% synthetic air, and 20% Ar, referred to as synthetic air, Ar, and mixed cover gas containing 4% CO_2 , respectively [9]. For each alloy, three parallel disc samples were heat-treated and later analyzed by Scanning Electron Microscope (SEM), Energy Dispersive X-ray Spectroscopy (EDS), and Electron Probe Micro Analyses (EPMA) to identify the surface morphology and the microstructure of the cross sections, as well as the chemical composition of the cross sections.

For the discs heat-treated in synthetic air, MgAl_2O_4 was established to have been formed in the case of the high Mg-containing Al alloy 5182, and MgO together with MgAl_2O_4 for the low Mg-containing Al alloy 6016. When heat-treated in pure Ar, however, a change in the elements present was observed for the Al alloy 5182 as only MgO was found to have been formed, however, both MgO and

Fig. 1 Sample preparation of heat-treated Al alloy discs, where **a** shows a cross section of a disc mounted in epoxy resin, and **b–d** show a sample mounted by clay in a deep sample holder (inner diameter 45 mm), seen from above, the side, and at an angled view



MgAl₂O₄ for the Al alloy 6016 were still present. For the disc samples heat-treated in the mixed cover gas containing 4% CO₂, it was difficult to establish a clear interphase between then top layers. It was, however, revealed higher concentrations of Mg and O close to the surface, but not on the very top surface, for both alloys. Based on the analyses, it was confirmed that small additions of CO₂ in an oxidizing atmosphere had an inhibiting effect on the oxidation rate in regard to the mass gain, as well as for the oxide layer thicknesses. It was challenging to investigate the overall mechanism of the inhibiting effect of the CO₂ and where the C had deposited due to the C-bonded chemicals in the epoxy resin used during sample preparations, see Fig. 1a. In the present study, other characterization techniques will therefore be applied trying to study how the CO₂ behaves for both Al alloy systems.

Experimental Procedure

X-Ray Diffraction (XRD)

All heat-treated Al discs from previous work [9] of both alloys were examined by a D8 A25 DaVinci X-Ray Diffractometer (Bruker, Billerica, Ma, USA) to verify and confirm the previously obtained results by micrographic analyses. The oxidized discs were mounted in a deep sample holder with the use of clay, and it was made sure that the surface was parallel to the edge of the sample holder, see Fig. 1b–d. Monochromatic CuK α photons with a wavelength of $\lambda = 1.54060 \text{ \AA}$ were used during the XRD scans. Each diffraction pattern was acquired with a step size of 0.013° and covered scattering angles 2θ over the range $10\text{--}85^\circ$. The TOPAS (v5, Bruker Billerica, Ma, USA) software was used for the refinement of the results, using the Powder Diffraction Files (PDFs) from the ICDD-4 + PDF-database.

Transmission Electron Microscopy (TEM)

The Al discs heat-treated in the mixed cover gas containing 4% CO₂, were further examined with the aim of identifying the role of CO₂ and its inhibiting effect on the rate of oxidation of Al alloys 5182 and 6016.

To avoid sample charging in the dual-beam Focused Ion Beam (FIB), a Cressington sputter coater was used to deposit a thin electrically conducting layer of Pt–Pd (80:20) on top of the Al alloy 5182 disc. No pre-coating was applied for the Al alloy 6016 disc sample. Subsequently, a Helios G4 UX FIB (FEI, Hillsboro, Or, USA) was used to prepare the TEM lamellae. The oxidized discs from both alloys were coated with two layers of C, of which the first layer was made by electron beam-assisted deposition, and the second by Ga⁺ ion-beam-assisted deposition. An accelerating voltage of 30 kV was initially applied during the coarse thinning. Final thinning was first done at 5 kV, before decreasing the voltage stepwise to 2 kV of either side of the TEM lamellae to minimize surface damage. Due to the characteristics of the precursor gas used during the carbon deposition, i.e. Naphthalene (C₁₀H₈), the amorphous carbon–hydrogen composite layer is easy to distinguish from any pure C layer that may originate from the CO₂ atmosphere.

A double spherical aberration-corrected Cold FEG JEOL ARM200FC microscope (JEOL Ltd., Tokyo, Japan), operated at 200 kV was used for the TEM analyses. Energy Dispersive X-ray Spectroscopy (EDS) and Electron Energy Loss Spectroscopy (EELS) were applied simultaneously using the Scanning Transmission Electron Microscopy (STEM) mode. The light elements such as C and O were better detected by EELS, while the heavier elements such as Al gave better results using the EDS. All STEM images were taken using a High-Angle Annular Dark-Field (HAADF) mode to secure both precision and accuracy of the profiling.

Table 1 Phases identified by X-Ray Diffraction (XRD) of aluminum (Al) alloys 5182 and 6016 heat-treated in three different cover gases

Al alloy	Cover gas	Phases present					
		Al	MgO	MgAl ₂ O ₄	Mg _{0.388} Al _{2.408} O ₄	Al ₂ O ₃	Mg ₂ C ₃
5182	(i) 80% synthetic air, 20% Ar	x	x	x	x	x	
	(ii) 99.999% Ar	x	x				
	(iii) 4% CO ₂ , 76% synthetic air, 20% Ar	x	x				x
6016	(i) 80% synthetic air, 20% Ar	x		x			
	(ii) 99.999% Ar	x	x	x		x	
	(iii) 4% CO ₂ , 76% synthetic air, 20% Ar	x	x	x			

Results and Discussion

Characterization by XRD

A complete overview of the phases identified by XRD for both Al alloys 5182 and 6016 in the case of all three cover gases used in the present study is presented in Table 1. As can be seen from the table, the XRD analyses confirm the observations from previous analyses obtained by EDS and EPMA reported elsewhere by the present authors [9].

For the high Mg-containing Al alloy 5182 heat-treated in synthetic air, MgO (magnesium oxide) and MgAl_2O_4 (spinel), as well as $\text{Mg}_{0.388}\text{Al}_{2.408}\text{O}_4$ (defect spinel) and Al_2O_3 (aluminum oxide), were identified to have been formed, and cubic MgO crystals and Al when heat-treated in Ar. It is believed that for the disc sample heat-treated in Ar, the oxidation process of MgO reached steady-state conditions, as the partial pressure of O_2 was not sufficient to cause breakaway oxidation at 750 °C when the holding time was restricted to 7 h, as seen for the disc sample heat-treated in synthetic air. For the disc sample heat-treated in the mixed cover gas containing 4% CO_2 , cubic MgO crystals were identified to have been formed by the XRD analysis, in addition to small amounts of Mg_2C_3 (magnesium carbide). It is in this case believed that a rougher surface with clear defects might have caused splitting of the CO_2 molecules and therefore caused Mg_2C_3 and O_2 to further react with the Mg vacancies present in the system forming other Mg, Al, and O containing phases. It was, however, not identified neither MgAl_2O_4 , $\text{Mg}_{0.388}\text{Al}_{2.408}\text{O}_4$ nor Al_2O_3 by the XRD to have been formed, which is believed to be due to the formation of a protective C layer resulting from the CO_2 present in the cover gas, delaying any diffusion of O_2 and potential oxidation reactions.

For the low Mg-containing Al alloy 6016 heat-treated in synthetic air, only MgAl_2O_4 was identified to have been formed, which is believed to be due to complete breakaway oxidation, i.e. the MgO from the first oxidation step continues to oxidize with Al forming MgAl_2O_4 . This correlates partly with previous findings, as no mapped areas with only Mg and O indicating the formation of MgO were reported from Solem et al. [9]. When heat-treated in Ar, however, MgO was detected together with MgAl_2O_4 and Al_2O_3 , indicating that the breakaway oxidation has partly occurred. For the disc sample heat-treated in the mixed cover gas containing 4% CO_2 , MgO and MgAl_2O_4 were identified to have been formed, revealing the absence of magnesium carbides. It is believed that all of the small amounts of Mg present in the alloy were oxidized and partly caused breakaway oxidation.

Due to the challenges with identifying the influence of CO_2 , further analysis of both Al alloys 5182 and 6016 discs

heat-treated in the mixed cover gas containing 4% CO_2 was carried out to investigate the layers and phases present.

Microscopy Analyses through TEM

To further evaluate the phases present in the oxidized Al alloy discs 5182 and 6016 heat-treated in the mixed cover gas containing 4% CO_2 , FIB followed by TEM and EDS-EELS analyses was carried out.

In Fig. 2a, the cross-section lamella made by FIB of the high Mg-containing Al alloy 5182 disc is presented. As can be seen from the figure, the deposited C layers, resulting from the sample preparation, were identified together with the Pt-Pd coating used to avoid sample charging. When looking further at the cross section of the sample itself, it is seen that there are MgO crystals (light gray crystals marked by purple box and arrows) present in the Al bulk (dark gray areas marked by green box). Closer to the surface, a dense, continuous nanocrystalline MgO layer can also be seen, confirming not only previously reported EDS and EPMA results [9, 10] but also the presently obtained XRD results.

On top of the nanocrystalline MgO layer, a thin continuous layer of amorphous C, which has never been previously observed, was detected, as seen in the TEM image in Fig. 2b, where the interface between the amorphous C layer and the nanocrystalline MgO layer is marked with a white solid line. The same C layer was found, but to a lesser extent for the low Mg-containing Al alloy 6016 disc. This correlates well with findings reported by the present authors and others, where it is believed that the CO_2 present in an oxidizing atmosphere may be absorbed on top of MgO crystals, and form a protective layer preventing further evaporation of the Mg and inhibiting the oxidation rate [10, 14].

STEM EDS-EELS analysis of the cross section was performed for both alloys to further evaluate the elements present in the oxide layers, as well as the C layer. A cross section of the Al alloy 5182 disc is presented in Fig. 3a, showing the HAADF STEM image of the Al bulk (bottom grey area), the nanocrystalline MgO layer covered by a continuous amorphous C layer, as well as the thin Pt-Pd coating (bright contrast layer on top of the amorphous C layer) and the protective C coating (black contrast due to the combination of the light elements of C and H). A combination of EDS and EELS analyses was used, where C, Mg, and O were mapped by EELS and Al by EDS.

Figure 3b–d shows the EDS-EELS results of the mapped elements of interest for the Al alloy 5182 disc. As can be seen in Fig. 3b from the mapping of C, a 40–100 nm continuous C layer is revealed close to and at the surface of the sample. As the HAADF STEM imaging procedure takes place with a contrast scale close to the atomic number

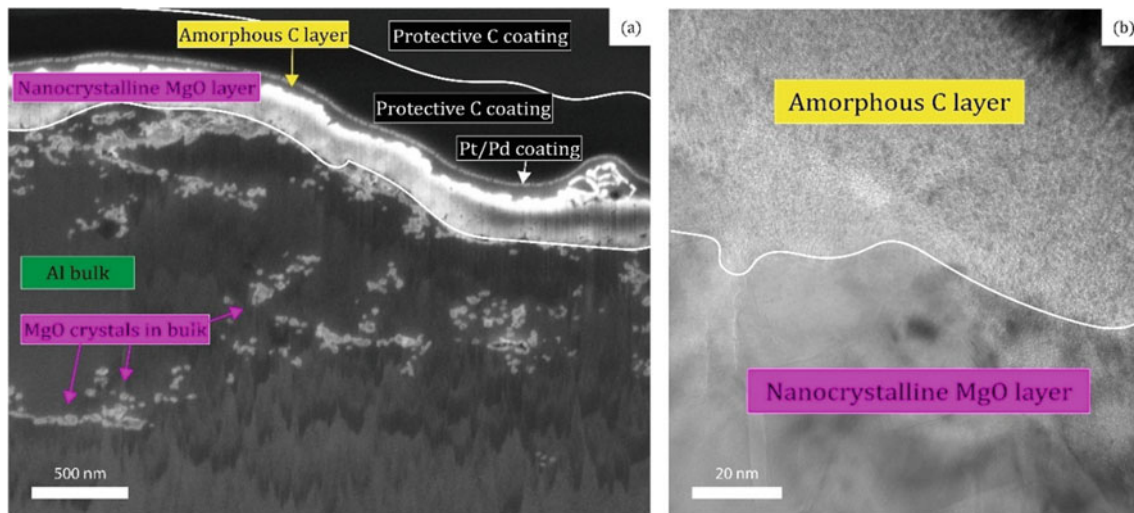


Fig. 2 Cross section of the Al alloy 5182 where **a** shows a Secondary Electron Microscopy (SEM) image of the disc sample after preparation by Focused Ion Beam (FIB), and **b** bright field Transmission Electron Microscopy (TEM) image of the interface between the amorphous C layer and the nanocrystalline MgO layer

squared, z_2 and the fact that the carbon protection layer consists of a mixture of hydrogen and carbon ($C_{10}H_8$), the deposited layer appears with a brighter contrast than the amorphous C layer that is originating from the sample surface itself. The EELS analyses of Mg and O presented in Fig. 3c and Fig. 3d, respectively, revealed the existence of a 200–400 nm thick layer of nanocrystalline MgO before reaching the Al bulk as seen in Fig. 3e. A heterogeneous distribution of MgO particles was also found to be present in the bulk of the disc sample.

With respect to the amorphous C layer on top of the nanocrystalline MgO layer, a similar layered structure was recognized for the low Mg-containing Al alloy 6016. A layer in the range of 15–120 nm of the thin amorphous C layer was identified on the top of a 160–200 nm thin nanocrystalline MgO layer. No individual MgO particles in the Al bulk were found to exist in the bulk of the disc sample, however, large ($\leq 2 \mu\text{m}$) $MgAl_2O_4$ particles were found by STEM-EELS-EDS close to the MgO layer as a discontinuous oxide layer.

Overall Discussion

Based on the presently obtained XRD and TEM results, it is believed that the amorphous nanometer-thin C layer, identified to exist for both Al alloy discs after heat-treated in a mixed cover gas containing 4% CO_2 , has an inhibiting effect on the rate of oxidation of both Mg and Al. The overall Mg concentration is also believed to play a key role in this process, as it clearly influences the thickness of the oxide layer, as well as the phases eventually formed.

Figure 3f summarizes the mapping of the Al alloy 5182 disc by color, where C, Mg, O, and Al are represented by the colors yellow, red, blue, and green, respectively, giving MgO the color of purple. As can be seen from the figure, the presence of the nanocrystalline MgO layer, as well as the MgO particles in the bulk, correlates well with the XRD results for the same sample, as only MgO was identified to have formed during heat treatment in the mixed cover gas containing 4% CO_2 . As for the Al alloy 6016 disc, $MgAl_2O_4$ was identified to have been formed by both XRD and TEM.

Moreover, the EELS analysis confirmed the formation of an amorphous nanometer-thin layer of C covering the nanocrystalline MgO layer. It is believed that the standard sample preparation technique applied and the use of epoxy resin containing C-bonded chemicals have made it difficult to identify the presence of the C layer during earlier investigations.

In the case of the Al alloy 6016, it is believed that the lower Mg concentration resulted in the formation of a thinner MgO layer. After reaching steady state conditions, the formation of $MgAl_2O_4$ took place, i.e. breakaway oxidation, before the amorphous C layer inhibited any further oxidation of MgO. As for the Al alloy 5182, the first oxidation step of Mg is believed not to have reached steady state before the inhibiting C layer was established, thus, no breakaway oxidation was identified to exist. Based on this, it is believed that for both Al alloys, the amorphous C layer formed on top of the MgO oxide layer seems to inhibit the evaporation of Mg, hence, delaying the overall rate of oxidation.

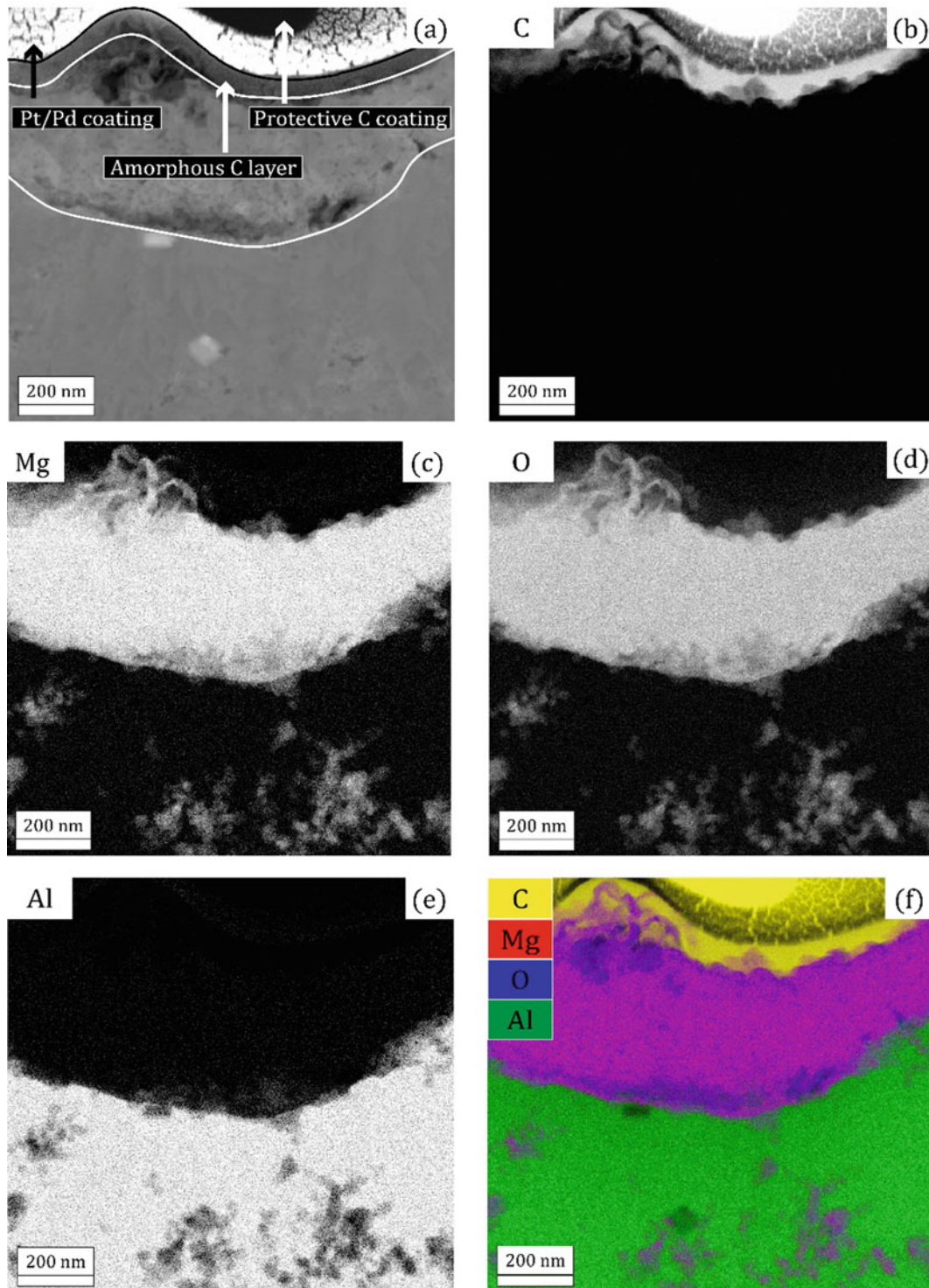


Fig. 3 a High-Angle Annular Dark-Field Scanning Transmission Electron Microscopy (HAADF STEM) image of the oxide layer of the Al alloy 5182 disc. The C b, Mg c, O d, and Al e mappings are made from the EELS-EDS spectroscopy maps. A combination of those various maps can be found in f

Conclusions

Oxidized discs of Al alloys 5182 (AlMg4.5Mn0.4) and 6016 (AlSi1.2Mg0.4), heat-treated in a gas mixture with 4% CO₂, 76% synthetic air, and 20% Ar at 750 °C for 7 h, have been analyzed by XRD and TEM to try to establish the inhibiting effect that CO₂ has on the oxidation process. The analyses revealed the presence of a 200–400 nm dense nanocrystalline MgO layer close to the surface of the high Mg-containing Al alloy 5182, covered by a 40–100 nm amorphous C layer. MgO crystals were also identified further into the Al bulk. Similar behavior was recognized for the low Mg-containing Al alloy 6016, having a nanocrystalline MgO layer of only 160–200 nm covered by a 15–120 nm-thin amorphous C layer. In this case, no MgO crystals were identified in the Al bulk of the disc sample, however, cubic MgAl₂O₄ crystals were found close to the MgO layer resulting in a discontinuous oxide layer in between the MgO layer and the Al bulk. In both cases, the amorphous C layer seems to hinder further evaporation of Mg delaying the rate of oxidation of Al and other alloying elements.

Future Work

The oxidized Al alloy 6016 discs will be further analyzed to clarify if there is a direct link between the Mg concentration and the thickness of the amorphous C- and nanocrystalline MgO layers, as indicated by the TEM results of the present study. X-Ray Photoelectron Spectroscopy (XPS) will also be used for both alloys, i.e. Al alloys 5182 and 6016, to construct a depth profile through the oxide layer towards the bulk. It is believed that this will allow a more detailed study of the C bonding in the amorphous layer, as well as the magnesium carbides identified for the high Mg-containing Al alloy 5182. Even further analysis and atomistic modelling will be performed to understand the mechanism of how the CO₂ interacts with the rough MgO surface.

Acknowledgements This work has been funded by the SFI Metal Production (Centre for Research-based Innovation, 237738). The authors gratefully acknowledge the financial support from the Research Council of Norway and the partners of the SFI Metal Production. The support from the Research Council of Norway to NORTEM (197405) and NorFab (245963/F50) is also acknowledged. Finally, the authors would also like to thank Egil Solberg from Alcoa ANS Mosjøen in Norway, for providing the Al alloy 5182 and 6016 samples.

References

1. Ingason HT, Sigfusson TI (2014) Processing of Aluminum Dross: The Birth of a Closed Industrial Process. *JOM* 66:2235–2242. <https://doi.org/10.1007/s11837-014-1156-z>
2. Gulbransen EA, Wysong WS (1947) Thin Oxide Films on Aluminum. *J Phys Chem* 51:1087–1103. <https://doi.org/10.1021/j150455a004>
3. More KL, Tortorelli PF, Walker LR, Hryn J, Krumdick G (2003) Microstructural Evaluation of Dross Formation on Mg- and Non-Mg-Containing Al Alloys from Industrial Furnaces. *Materials at High Temperatures*; Leeds 20:453. <https://doi.org/10.3184/096034003782748838>
4. Kim K (2015) Formation of Endogenous MgO and MgAl₂O₄ Particles and their Possibility of Acting as Substrate for Heterogeneous Nucleation of Aluminum Grains. *Surface and Interface Analysis* 47:429–438. <https://doi.org/10.1002/sia.5726>
5. Drieling H, Chesonis DC (2016) The Effect of Magnesium Supply on the Quality of Aluminum Melts. In: Grandfield J (ed) *Light Metals 2014*. Springer International Publishing, Cham, pp 1071–1075
6. Smith N, Kvithyld A, Tranell G (2018) The Mechanism Behind the Oxidation Protection of High Mg Al Alloys with Beryllium. *Metall and Materi Trans B* 49:2846–2857. <https://doi.org/10.1007/s11663-018-1340-6>
7. Cochran CN, Belitskus DL, Kinosz DL (1977) Oxidation of Aluminum-Magnesium Melts in Air, Oxygen, Flue Gas, and Carbon Dioxide. *MTB* 8:323–332. <https://doi.org/10.1007/BF02657663>
8. Solem CKW, Ekstrøm KE, Tranell G, Aune RE (2020) Evaluation of the Effect of CO₂ Cover Gas on the Rate of Oxidation of an AlMgSi Alloy. In: Tomsett A (ed) *Light Metals 2020*. Springer International Publishing, Cham, pp 1141–1147
9. Solem CKW, Solberg E, Tranell G, Aune RE (2021) Influence of Mg Concentration on the Inhibiting Effect of CO₂ on the Rate of Oxidation of Aluminum Alloys 5182 and 6016. *Light Metals 2021*:742–750. https://doi.org/10.1007/978-3-030-65396-5_97
10. Smith N, Gleeson B, Saidi WA, Kvithyld A, Tranell G (2019) Mechanism Behind the Inhibiting Effect of CO₂ on the Oxidation of Al–Mg Alloys. *Ind Eng Chem Res* 58:1434–1442. <https://doi.org/10.1021/acs.iecr.8b04691>
11. Qu Q, Ma J, Wang L, Li L, Bai W, Ding Z (2011) Corrosion Behaviour of AZ31B Magnesium Alloy in NaCl Solutions Saturated with CO₂. *Corrosion Science* 53:1186–1193. <https://doi.org/10.1016/j.corsci.2010.12.014>
12. Tosoni S, Spinnato D, Pacchioni G (2015) DFT Study of CO₂ Activation on Doped and Ultrathin MgO Films. *J Phys Chem C* 119:27594–27602. <https://doi.org/10.1021/acs.jpcc.5b10130>
13. Toda Y, Hirayama H, Kuganathan N, Torrisi A, Sushko PV, Hosono H (2013) Activation and Splitting of Carbon Dioxide on the Surface of an Inorganic Electride Material. *Nat Commun* 4:2378. <https://doi.org/10.1038/ncomms3378>
14. Haginoya I, Fukusako T (1983) Oxidation of Molten Al–Mg Alloys. *Trans JIM* 24:613–619. <https://doi.org/10.2320/matertrans1960.24.613>